

An improved Mesri creep model for unsaturated weak intercalated soils

ZHU Yan-bo(祝艳波)^{1,2}, YU Hong-ming(余宏明)¹

1. Faculty of Engineering, China University of Geosciences, Wuhan 430074, China;
2. College of Geology Engineering and Geomatics, Chang'an University, Xi'an 710054, China

© Central South University Press and Springer-Verlag Berlin Heidelberg 2014

Abstract: The weak intercalated soils in redbed soft rocks of Badong formation have obvious creep characters. In order to predict the unsaturated creep behaviors of weak intercalated soils, an unsaturated creep model was established based on the unsaturated creep tests of weak intercalated soils by using GDS triaxial apparatus. The results show that the creep behaviors of intercalated soils are apparent and significantly affected by matric suction. Based on this, an empirical Mesri creep model for intercalated soils under varying matric suction was built. The fitting results show that the parameters E_d and m of this model are in good power relations with matric suction s and stress level D_r , respectively. An improved Mesri creep model was established involving stress–matric suction–strain–time, which is more precise than the Mesri creep model in predicting the unsaturated creep behaviors of weak intercalated soils.

Key words: unsaturated soils; creep; matric suction; improved Mesri model

1 Introduction

Yichang–Badong highway partially passes through the purplish red soft rock strata of Badong formation (T_2b^2), and weak intercalations are outcropped in some of the cutting slopes formed along the highway. The rheological properties of weak intercalated soils have been indicated in numerous studies [1–5]. As side slopes are dug out, the weak intercalated soils will be subjected to a different stress status and thereby creep to some extent. The mechanical properties of intercalated soils show the strength damage accumulation effect and the time effect, which are extremely unfavorable for the stability of cutting slopes.

Previous studies on the creep characteristics of soils mostly focus on saturated state. In fact, at most time, natural weak intercalated soils in this area are under unsaturated state with certain matric suction, which affects the deformation properties of intercalated soils. Therefore, studying the unsaturated creep characters and establishing a creep model to forecast the unsaturated creep behaviors of weak intercalated soils will be significant for engineering practice.

So far, there are many models elaborating the creep behaviors of soils [6–9]. Generally, the stress–strain relationship is expressed by a hyperbolic function [10] and the strain–time relationship is expressed by a power function [11–12]. Among these models, the two widely used empirical models are Mesri model and Singh–

Mitchell model [13–14], especially Mesri model [15–16] which is independent of stress level. These two models have also been improved later [17–18] and then applied in engineering practice. However, these creep models mostly focus on the creep behaviors of saturated soils, but rarely on the unsaturated soils. An unsaturated visco-elastoplastic model was constructed by PRIOL et al [19] based on an unsaturated elastoplastic model [20] and through triaxial creep tests for unsaturated chalky soils. Based on unsaturated triaxial creep tests for a landslide sliding zone, an unsaturated creep model considering matric suction was built [21–22].

In this work, targeting at the exposed weak intercalated soils in cutting slopes, the unsaturated creep tests were performed by using a GDS unsaturated triaxial apparatus. Based on the empirical Mesri creep model, an unsaturated creep model involving stress–matric suction–strain–time was built, which forecasts the unsaturated creep behaviors of intercalated soils better.

2 Unsaturated creep tests for intercalated soil

2.1 Creep tests

Soils were sampled from the outcropped weak intercalated soils in some cutting slopes along the Yichang–Badong highway. The physical properties of the purplish red soils were measured by laboratory tests and mineral identification (Table 1). Then, the soils were made into remolded samples with density of 1.85 g/cm^3

Foundation item: Project supported by Science & Technology Program of Hubei Traffic and Transport Office, China; Project(41272377) supported by the National Natural Science Foundation of China

Received date: 2013–08–26; **Accepted date:** 2014–09–09

Corresponding author: ZHU Yan-bo, PhD; E-mail: zhuyanbobd@126.com

Table 1 Physical indexes of weak intercalation soils in soft rocks of Badong formation

Dry density, $\rho_d/(g \cdot cm^{-3})$	Specific gravity, C_s	Natural water content, $W/\%$	Liquid Plastic limit, $W_L/W_p/\%$		Grain composition						Primary mineral composition
			$W_L/\%$	$W_p/\%$	<5 mm	<2 mm	<1 mm	<0.5 mm	<0.25 mm	<0.075 mm	
1.85	2.67	11.3	25.8	13.57	0	23.16	30.02	12.61	18.18	16.03	Montmorillonite, chlorite, quartz

and water content of 15%.

A GDS unsaturated triaxial test system [23–25] was used to conduct the unsaturated creep tests. Step load was used in this test. With the unsaturated test module, triaxial creep tests for unsaturated intercalated soils were conducted under the net peripheral pressure of 100 kPa and the matric suctions of 100 kPa, 200 kPa, 300 kPa and 400 kPa.

2.2 Test results

The creep tests of intercalated soils under four different matric suctions were conducted within 1 a. CHEN and KANG’s method [26] was used in the nonlinear superposition of the step-loaded creep curves, and thereby the stress–strain–time creep curves under varying matric suction were obtained. In this work, the experimental curves and analytical results of samples only under matrix suction of 200 kPa were given. Figure 1 shows the creep curves under matric suctions of 200 kPa.

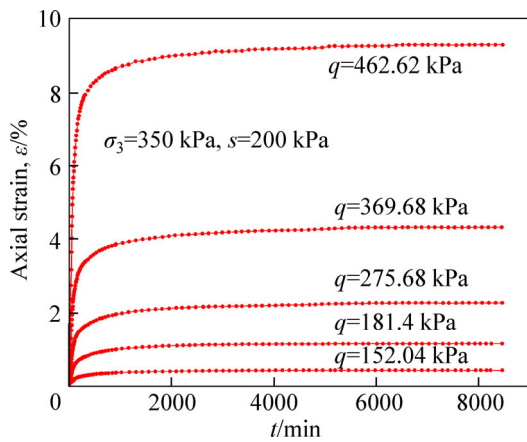


Fig. 1 Creep test curves of intercalated soil sample under matric suction of 200 kPa

Then, the isochronous stress–strain curves under matric suction of 200 kPa were plotted (Fig. 2). The curves are apparently nonlinear. With elevated deviator stress, the creep strain grows in an accelerated nonlinear way, and this growing trend is intensified with time. Figure 3 shows the isochronous stress–strain curves under different matric suctions. Obviously, under the same deviator stress, the creep strain is enhanced with the decrease of matric suction. Namely, when deviator stress is invariable, higher water content results in more serious deformation, which is more obvious at higher

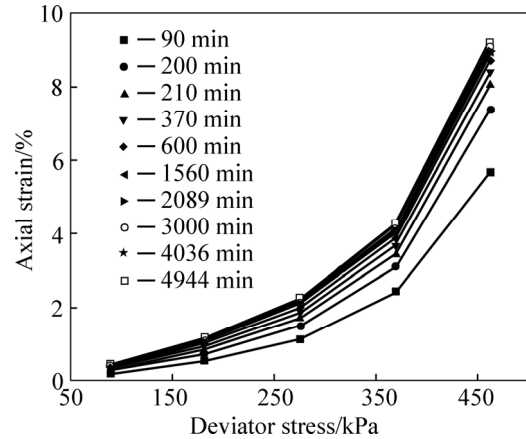


Fig. 2 Isochronous curves of intercalated soil samples under $s=200$ kPa

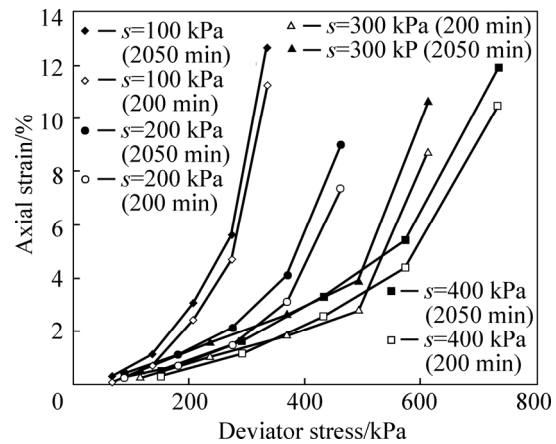


Fig. 3 Isochronous curves of intercalated soil samples under different matric suctions

stress level. A higher deviator stress results in a higher creep strain when the matric suction is invariable.

3 Mesri creep model

3.1 Mesri creep model

In the Mesri creep model, the stress–strain relationship is expressed by a hyperbolic function, and the strain–time relationship is expressed by a power function [14]. The model is expressed as follows:

$$\varepsilon = \left[\frac{(\sigma_1 - \sigma_3)_f}{E_d} \right]_t \frac{D_t}{1 - (R_f)_t D_t} \left(\frac{t}{t_0} \right)^m \tag{1}$$

where ε is creep strain; $(\sigma_1 - \sigma_3)_f$ is damage deviator stress, kPa; E_d is the initial tangent modulus of the creep curve,

MPa; D_r is deviator stress level; R_f is damage ratio, which is the averaged slope of $\varepsilon/D_r-\varepsilon$ curves at different time points; t_0 is reference creep time and the strain at t_0 is used as the initial creep strain. Based on the creep curves for unsaturated intercalated soils, on the time needed to impose deviator stress and on the initial creep strain after imposition, t_0 is determined to be 90 min. m is the mean slope of $\ln\varepsilon-\ln t$ curves under different stress levels.

3.2 Solving parameters of Mesri model

3.2.1 Strain–time relationship

In the Mesri creep model, the parameter m is independent of time if the effects of stress level are ignored. Then, the $\ln\varepsilon-\ln t$ relation curves under different matric suctions and different stress levels are plotted and linearly fitted. The slopes of straight lines are the values of m_r under different stress levels, and the slopes are averaged to obtain the value of m . The calculated results are listed in Table 2. Because of limited space, the $\ln\varepsilon-\ln t$ curves of weak intercalation sample only under $s=200$ kPa are shown in this work (Fig. 4).

Table 2 Parameters of Mesri creep model

s/kPa	m	R_f	$(\sigma_1-\sigma_3)_f/E_d$	E_d/MPa
100	0.1520	1.0387	0.01127	34.2441
200	0.1272	0.9424	0.01399	39.5085
300	0.1392	0.8895	0.01673	42.2670
400	0.1122	0.9589	0.02035	42.6133

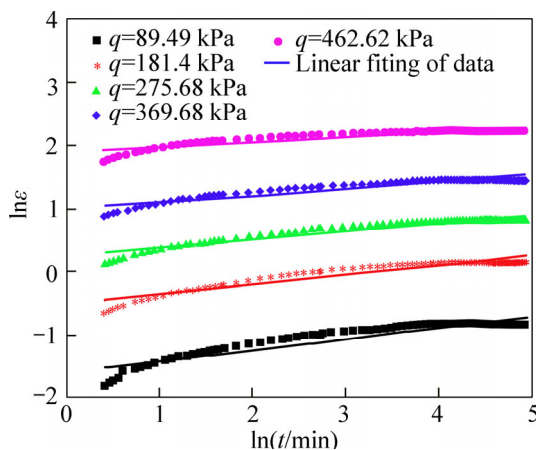


Fig. 4 $\ln\varepsilon-\ln t$ relation curves of intercalated soil sample when $\sigma_3=350$ kPa and $s=200$ kPa

3.2.2 Stress–strain relationship

In the Mesri creep model, the stress–strain relationship is expressed by a hyperbolic function, with the assumption that R_f and $(\sigma_1-\sigma_3)_f/E_d$ are independent of stress level and time. The $\varepsilon/D_r-\varepsilon$ curves under different matric suctions and at different time points are plotted. Because of limited space, Figure 5 shows the $\varepsilon/D_r-\varepsilon$

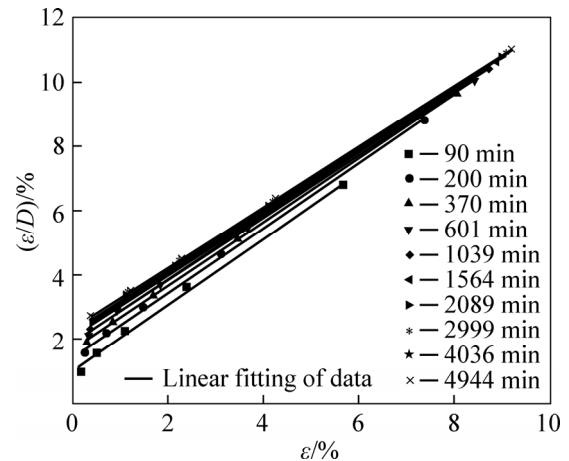


Fig. 5 Isochronous $\varepsilon/D-\varepsilon$ curves at different time points when $\sigma_3=350$ kPa and $s=200$ kPa

curves of intercalated soil sample at different time points only under $s=200$ kPa. The curve is linearly fitted, where R_f is slope and $[(\sigma_1-\sigma_3)_f/E_d][t/t_0]^m$ is intercept. Then the means are used as the values of the parameters in the Mesri model, and the calculated results are listed in Table 2.

Then, the creep forecast curves are plotted with these values. The calculated results are compared with the test results. Figure 6 shows the creep comparison curves of intercalated soil sample under $s=200$ kPa. The results show that the Mesri model is not effective at prediction, and at higher stress level, the forecast results deviate from the test results more severely. Such deviation caused by the parameter m , which expresses the creep curve's slope, is the average slope of $\ln\varepsilon-\ln t$ lines under different stress levels. However, m is associated with stress level [27]. The method of using the mean m in the creep curves under different stress levels is not appropriate and thus the precision of forecast is not high.

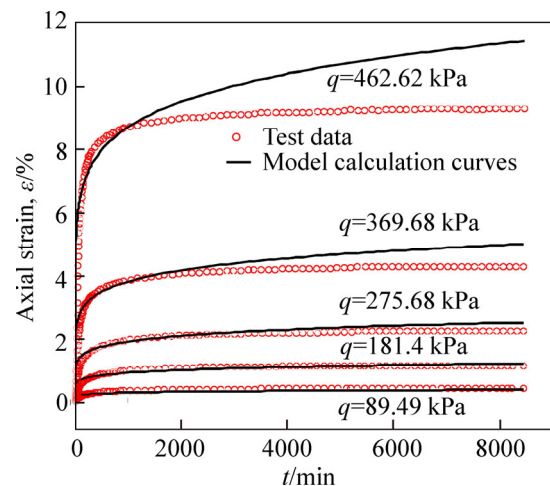


Fig. 6 Comparison of calculated results of Mesri model and test results when when $\sigma_3=350$ kPa and $s=200$ kPa

4 Improved Mesri model

4.1 Construction of improved Mesri model

In the Mesri creep model, only the stress–strain–time relationship is built. However, regarding the creep of unsaturated soils, a new variable of matric suction should be added. Therefore, an unsaturated creep model with stress–matric suction–strain–time is constructed. JANBU [28] pointed out that the initial tangent modulus E_d is a power function of peripheral pressure σ_3 . Based on this, $E_d-(s/p_a)$ relation curve is plotted. As shown in Fig. 7, the relationship between E_d and matric suction s is analyzed and built. Then, the data points are nonlinearly fitted. The results show that their relationship can be expressed by a power function as follows:

$$E_d = Ap_a (s / p_a)^n \tag{2}$$

where atmospheric pressure $p_a=101.33$ kPa; A and n are the material constants and can be determined from the fitted power function of $E_d-(s/p_a)$. The improved Mesri model can be built by substituting Eq. (2) into the Mesri model as follows:

$$\varepsilon = \left[\frac{(\sigma_1 - \sigma_3)_f}{Ap_a (s / p_a)^n} \right]_r \frac{D_r}{1 - (R_f)_r D_r} \left(\frac{t}{t_0} \right)^m \tag{3}$$

where the symbols are the same as those in Eqs. (1) and (2).

In Eq. (3), a new variable of matric suction is added, which considers the effects of water content on creep behaviors. With A and n , the matric suction is substituted into Eq. (2) to obtain E_d at each matric suction, and thereby $(\sigma_1 - \sigma_3)_f/E_d$ is obtained. The parameters of the improved model are listed in Table 3.

After analyzing the relationship between m_r under different stress levels and the corresponding stress level, it is found that m_r is associated with stress level. Then, their relation curve is plotted in Fig. 8 and the relation is

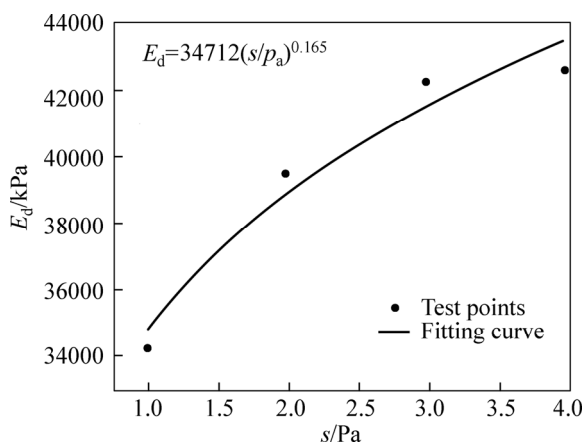


Fig. 7 Relationship between matric suction s and initial tangent modulus E_d with $R^2=0.960$, $A=343.68$ and $n=0.165$

Table 3 Parameters of stress–matric suction–strain–time model

s/kPa	m	R_f	$(\sigma_1 - \sigma_3)_f/E_d$	E_d/MPa
100	0.1520	1.0387	0.01114	34.6551
200	0.1272	0.9424	0.01423	38.8541
300	0.1392	0.8895	0.01702	41.5424
400	0.1122	0.9589	0.01990	43.5619

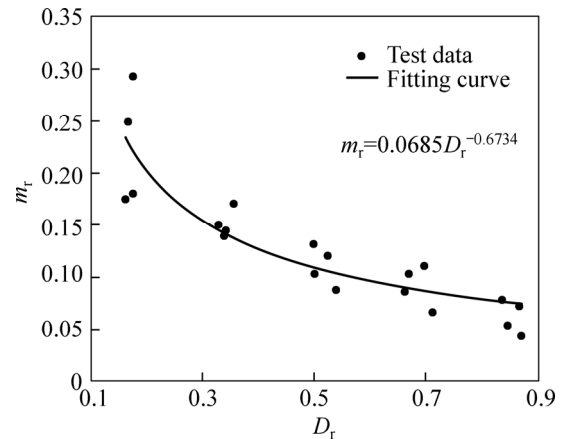


Fig. 8 Relation curve of m_r and D_r

fitted to be

$$m_r = aD_r^b \tag{4}$$

where $a=0.0685$ and $b=-0.6764$ are material constants and are obtained from the fitted curve of m_r and D_r . The improved unsaturated Mesri model can be built by substituting Eq. (4) into Eq. (3) as follows:

$$\varepsilon = \left[\frac{(\sigma_1 - \sigma_3)_f}{Ap_a (s / p_a)^n} \right]_r \frac{D_r}{1 - (R_f)_r D_r} \left(\frac{t}{t_0} \right)^{aD_r^b} \tag{5}$$

4.2 Model validation

In comparison of the calculated results with the test results (Fig. 9), the improved Mesri creep model is apparently more precise than the Mesri model in

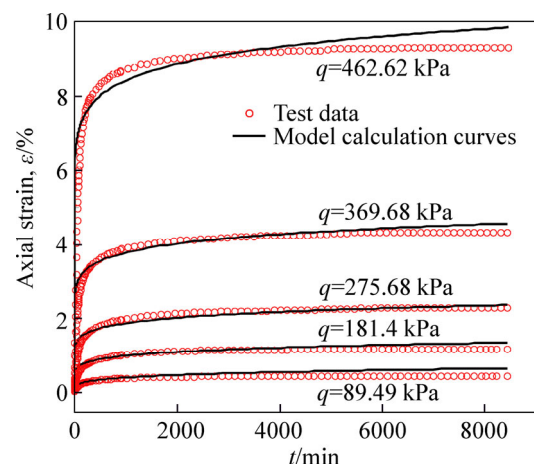


Fig. 9 Comparison of calculated results of improved Mesri model and test results when $\sigma_3=350$ kPa and $s=200$ kPa

predicting the creep behaviors of intercalated soils. This is because in the improved model, the slope of the forecast curve at each stress level is calculated from $\ln \varepsilon - \ln t$ curve under the corresponding stress level, which more really reflects the creeping speed. Though at low and high stress levels, the improved Mesri model deviates from the test results to some extent, its forecast precision satisfies requirements for engineering application, combined with the stress status of practical engineering in real intercalated soils.

5 Conclusions

1) An improved Mesri creep model is established based on the power relations of model parameter E_d and matric suction, model parameter m and stress level. The improved Mesri model is not only an unsaturated creep model involving stress–matric suction–strain–time, but also associates the creep speed with stress level.

2) The comparison of model calculated results and test results shows that the effect of the improved Mesri creep model in predicting the unsaturated creep behaviors of weak intercalated soils is better. The improved Mesri creep model can be used to predict the long-term creep behaviors of weak intercalation soils in soft rocks for analyzing the stability of this type cutting slopes. The study will provide a new clue for investigating how creep behaviors of intercalated soils affect the stability of cutting slopes from aspect of unsaturated soils.

References

- [1] LI Ke-ri, KANG Wen-fa. Creep testing of thin interbedded clayey seams in rock and determination of their long-term strength [J]. *Rock and Soil Mechanics*, 1983, 4(1): 39–45.
- [2] ZHANG Qi-hua, PENG Guang-zhou. Research on creep behavior of the weak intercalated bed in the dangerous rock body of Lianzi Cliff [J]. *Rock and Soil Mechanics*, 1997, 18(1): 60–64.
- [3] WANG Zhi-jian, YIN Kun-long, JIAN Wen-xing. Experimental research on creep of incompetent beds in Jurassic red clastic rocks in Wanzhou [J]. *Rock and Soil Mechanics*, 2007, 28(s1): 40–44.
- [4] YANG Tian-hong, RUI Yong-qin, ZHU Wan-cheng, SHEN Li, LIU Jing-hui, YANG Hong-kei. Rheological characteristics and long-term strength of siltized intercalation interbedded in Peat mudstone [J]. *Journal of Experimental Mechanics*, 2008, 23(5): 398–402.
- [5] CHENG Qiang, ZHOU De-pei, FENG Zhi-jun. Research on shear creep property of typical weak intercalation in redbed soft rock [J]. *Chinese Journal of Rock Mechanics and Engineering*, 2009, 28(s1): 3176–3180.
- [6] BISHOP A W, LOVENBURY H T. Creep characteristics of two undisturbed clays [C]// *Proc 7th ICSMFE*. Mexico, 1969: 29–37.
- [7] VAID Y P, CAMPANELLA R G. Time-dependent behavior of undisturbed clay [J]. *J Geotech Eng*, 1977, 103(7): 693–709.
- [8] AUGUSTESEN A, LIINGAARD M, LADE P V. Evaluation of time-dependent behavior of soils [J]. *Int J Geomech*, 2004, 4(3): 137–156.
- [9] LIINGAARD M, AUGUSTESEN A, LADE P V. Characterization of models for time-dependent behavior of soils [J]. *Int J Geomech*, 2004, 4(3): 157–177.
- [10] CHARLES J A. Geotechnical properties of coarse grained soils [C]// *Proc of 12th Int Conf Soil Mech Found Engng*. Riode Janeiro, 1989: 2495–2519.
- [11] SINGH A, MITCHELL J K. General stress–strain–time function for soils [J]. *Journal of Soil Mechanics and Found Engineering Division, ASCE*, 1968, 94(1): 21–46.
- [12] MESRI G, REBRES-CORDERO E, SHIELDS D R. Shear stress–strain–time behavior of clays [J]. *Geotechnique*, 1981: 31(4): 537–552.
- [13] SINGH A, MITCHELL J K. General stress–strain–time function for soils [J]. *Journal of Soil Mechanics and Found Engineering Division, ASCE*, 1968, 94(1): 21–46.
- [14] MESRI G, REBRES-CORDERO E, SHIELDS D R. Shear stress–strain–time behavior of clays [J]. *Geotechnique*, 1981: 31(4): 537–552.
- [15] LI Shi-jun, SUN Jun. Mesri's Creep model for shanghai silt-clay [J]. *China Civil Engineering Journal*, 2001, 34(6): 74–79.
- [16] CHEN Jing-jing, LIU De-fu, WANG Shi-mei. Mesri's creep model for Qingjiang Landslide-zone Soil [J]. *Journal of University of Hydraulic and Electric Engineering*, 2005, 27(1): 16–19.
- [17] WANG Chen, ZHANG Yong-li, LIU Hao-wu. A modified Singh-Mitchell's creep function of sliding zonesoils of Xietan landslide in Three Gorges [J]. *Rock and Soil Mechanics*, 2005, 26(6): 415–418.
- [18] WANG Chen, LIU Hao-wu, XU Qiang. Modified mesrips creep model for soils in sliding zone of xietan landslide in the three gorges [J]. *Journal of Southwest Jiaotong University*, 2004, 39(1): 15–19.
- [19] PRIOL G, DE GENNARO V, DELAGE P. Experimental investigation on the time dependent behaviour of a multiphase chalk [C]// *Proceedings of 2nd International Conference on Mechanics of Unsaturated Soils*. Weimar: Bauhaus Univ Weimar, 2007: 161–167.
- [20] ALONSO E E, GENS A, JOSA A. A constitutive model for partially saturated soils [J]. *Geotechnique*, 1990, 40(3): 405–430.
- [21] LAI Xiao-ling, LIU Yin, QIN Hong-bin. Unsaturated creep model of the sliding zone soils of Qianjiangping landslide in Three Gorges [J]. *Disaster and Control Engineering*, 2009(1): 41–46.
- [22] LAI Xiao-ling, YE Wei-min, WANG Shi-mei. Experimental study on unsaturated creep characteristics of landslide soils [J]. *Chinese Journal of Geotechnical Engineering*, 2012, 34(2): 286–293.
- [23] ZHAN Liang-tong. Field and laboratory study of an unsaturated expansive soil associated with rain-induced slope instability [D]. Hong Kong: The Hong Kong University of Science and Technology, 2003.
- [24] ZHAN Liang-tong, NG C W W. Experimental study on mechanical behavior of recompacted unsaturated expansive clay [J]. *Chinese Journal of Geotechnical Engineering*, 2006, 28(2): 196–201.
- [25] ZHU Yan-bo, YU Hong-ming, GAO Jian-wei. Experimental study on deformation and strength of Badong unsaturated red clay [J]. *Journal of Engineering Geology*, 2012, 20(6): 1050–1056.
- [26] TAN Tjong-kie, KANG Wen-fa. On the locked in stress, creep and dilatation of rocks, and the constitutive equations [J]. *Chinese Journal of Rock Mechanics and Engineering*, 1991, 4: 299–312.
- [27] WANG Zhi-jian. Rheological experimental study and mechanism research on gentle-dipped landslides of jurassic red strata in wanzhoucity [D]. Wuhan: Chinese university of Geosciences, 2008.
- [28] JANBU N. Soil compressibility as determined by oedometer and triaxial tests [C]// *Proceedings of European Conference on Soil Mechanics and Foundation Engineering*. Wiesbaden, 1963: 19–25.

(Edited by FANG Jing-hua)